MODELING FLOWS AROUND MERGING BLACK HOLE BINARIES

JAMES R. VAN METER[1], JOHN H. WISE[2], M. COLEMAN MILLER[3,4], CHRISTOPHER S. REYNOLDS[3,4], JOAN CENTRELLA[1],
JOHN G. BAKER[1], WILLIAM D. BOGGS[1,5], BERNARD J. KELLY[1], AND SEAN T. MCWILLIAMS[1]
[1] Gravitational Astrophysics Laboratory, NASA Goddard Space Flight Center, Greenbelt, MD 21114, USA; james.r.vanmeter@nasa.gov
[2] Laboratory for Observational Cosmology, NASA Goddard Space Flight Center, Greenbelt, MD 21114, USA
[3] Department of Astronomy, University of Maryland, College Park, MD 20742, USA
[4] Joint Space Science Institute, University of Maryland, College Park, MD 20742, USA
[5] Department of Physics, University of Maryland, College Park, MD 20742, USA

ABSTRACT

Coalescing massive black hole binaries are produced by the mergers of galaxies. The final stages of the black hole coalescence produce strong gravitational radiation that can be detected by the space-borne *Laser Interferometer Space Antenna*. In cases where the black hole merger takes place in the presence of gas and magnetic fields, various types of electromagnetic signals may also be produced. Modeling such electromagnetic counterparts of the final merger requires evolving the behavior of both gas and fields in the strong-field regions around the black holes. We have taken a step toward solving this problem by mapping the flow of pressureless matter in the dynamic, three-dimensional general relativistic spacetime around the merging black holes. We find qualitative differences in collision and outflow speeds, including a signature of the merger when the net angular momentum of the matter is low, between the results from single and binary black holes, and between nonrotating and rotating holes in binaries. If future magnetohydrodynamic results confirm these differences, it may allow assessment of the properties of the binaries as well as yielding an identifiable electromagnetic counterpart to the attendant gravitational wave signal.

Key words: black hole physics – galaxies: nuclei – gravitational waves

Online-only material: color figures

1. INTRODUCTION

Electromagnetic signatures of the coalescence of two supermassive black holes would, in concert with the detection of gravitational waves from the event, allow a high-precision determination of both the redshift and the luminosity distance to the merger. This would provide a precise probe of cosmology, limited mainly by uncertainties in the magnification, and hence the luminosity distance, due to weak gravitational lensing (Hughes & Holz 2003). As a result, there has been substantial recent interest in mechanisms that could produce electromagnetic emission from a surrounding accretion disk (Armitage & Natarajan 2002; Milosavljević & Phinney 2005; Dotti et al. 2006; Kocsis et al. 2006; Phinney 2007, 2009; Chang et al. 2009; Bode & Phinney 2007; Shields & Bonning 2008; Lippai et al. 2008; Schnittman & Krolik 2008; Kocsis & Loeb 2008; Kocsis et al. 2008; Haiman et al. 2009a; Haiman et al. 2009b; O'Neill et al. 2009; Megevand et al. 2009). However, there have been relatively few investigations of the electromagnetic signatures that could emerge from the dynamic spacetime near the binary during its last few orbits (for a recent exception, see Palenzuela et al. 2009).

There are reasons to believe that if significant gas exists around the binary in its last few orbits, then intense but short-lived electromagnetic signals will be produced. For example, since the binary orbital speed can be half the speed of light or more, even in the Newtonian case the slingshot mechanism could be particularly effective in ejecting matter or producing collisions that have a high Lorentz factor. In addition, it has been proposed that magnetic fields in the vicinity of the orbit could be wound up and amplified to such a degree that they would produce a strong Poynting outflow (R. Blandford 2008, private communication). Exploration of such effects would require simulations that involve magnetohydrodynamics (MHD) in a dynamical spacetime.

Here we take a step toward such simulations by tracing the paths of pressureless test particles (i.e., particles of non-zero rest mass in geodesic motion) in the dynamical spacetime of coalescing black holes. Our goal is to determine whether the outflows and collisions are sufficiently high speed, compared with the equivalents around a single black hole that unique signatures of the binary motion seem plausible. This will pave the way for the extensive development required to do a full analysis of MHD in a dynamical spacetime. In Section 2, we discuss our simulation setup, which uses a code that has been used to model successfully the coalescence of black holes of different masses, spin magnitudes, and orientations. We choose units in which $c = 1$ and $G = 1$; with this, the total mass M is related to time and distance by $M \sim 5 \times 10^{-6}\,(M/M_\odot)$ s $\sim$ 1.5 $(M/M_\odot)$ km. In Section 3, we present and discuss our results, in which we examine first the coalescence of equal-mass nonspinning black holes and then show that equal-mass black holes with aligned spins produce significantly more extreme effects.

2. SIMULATION SETUP

In the following simulations, the spacetime was computed by solving Einstein's field equations using finite differencing methods of numerical relativity (Imbiriba et al. 2004; Baker et al. 2008). On the initial slice, the black holes are represented by "punctures" (Brandt & Brügmann 1997), and the constraint equations are solved using a multigrid solver (Brown & Lowe 2005). The black holes are then evolved forward in time by integrating the time-dependent Einstein equations given by the BSSN formulation (Shibata & Nakamura 1995; Baumgarte & Shapiro 1998). We use coordinate conditions that allow the black holes to move freely across the grid (Baker et al. 2006; Campanelli et al. 2006; van Meter et al. 2006). Meanwhile, the test matter is modeled by non-interacting point particles.

To evolve the test matter, we integrate the geodesic equation for each particle in this spacetime. The metric at the location of each particle is obtained by interpolation from the computational grid.

The geodesic code was tested for a variety of trajectories around a single black hole, both spinning and nonspinning. For coordinate conditions in which the conversion to Boyer–Lindquist coordinates was known, the particle worldline was compared with independent calculations and found to be at least fourth-order convergent in the grid spacing, as were the constants of motion, energy (E), angular momentum (L), and Carter's constant (Q). For the coordinate conditions closer to those of our typical binary black hole runs, the constant of motion L, readily calculable in any axisymmetric coordinate system, was still found to be at least fourth-order convergent.

Initial data for the spacetime background used here were chosen to represent two black holes, each of mass $m = M/2$, in nearly circular inspirals. In our simulations, the black holes were either spinless, or were each given a spin of $a/m = 0.8$, aligned with the orbital angular momentum. The initial linear momenta of the black holes were given by the post-Newtonian approximation, and the initial separation of the black holes was chosen so as to give at least five orbits before merger. As a control case, we have also run equivalent simulations with a single isolated nonrotating black hole of mass M.

In these spacetimes, approximately 75,000 geodesic particles were initially distributed uniformly throughout a solid annulus of inner radius $8\,M$, outer radius $25\,M$, and vertical full thickness $10\,M$. We excluded particles within the inner radius to avoid transient signatures from particles initially near the horizons. We have chosen such a geometrically thick disk because these are the disks that potentially have high enough inward radial speeds to keep up with the shrinking binary, as opposed to being stranded at large radii as the binary coalesces (see Milosavljević & Phinney 2005).

We explored two initial velocity configurations for the particles. In the first configuration ("orbital"), the initial velocities are randomly distributed (with velocity components drawn from a Gaussian distribution) around a tangential velocity V_c that would give a circular orbit in a Schwarzschild spacetime of mass M, resulting in a scale height of $5\,M$. In the second configuration ("isotropic"), we consider an extreme case where the particles only have random velocities, with each component sampled from a Gaussian distribution of standard deviation $V_c/\sqrt{3}$.

We choose these two configurations in order to (within the limitations of our test-particle framework) bracket the realistic flow. Circumbinary matter will be distributed in a rotationally supported accretion disk, but fluid processes (most notable the magneto-rotational instability; Balbus & Hawley 1991) will lead to angular momentum redistribution and hence inflow inward the binary. Furthermore, if the inner regions of this accretion disk are sufficiently tenuous, the flow may be radiatively inefficient (Ichimaru 1977; Rees et al. 1982; Narayan & Yi 1994). This, in turn, would produce a disk that has an ion temperature close to viral, is geometrically thick, and has strong inflows.

We output the positions and proper 4-velocities of the particles every $\sim 1\,M$ and $\sim 0.5\,M$ in the nonrotating and rotating cases, respectively. Particles within an apparent horizon are discarded. We then search for and characterize "collisions" between test particles; we define a particle collision as two particles traveling within $r_c = 0.1\,M$ of each other, assuming that they travel on straight lines between successive output times. We have found that the collision energies are not sensitive to r_c in the range

of 0.01–$1\,M$. For every particle, we search the nearest eight neighbors for any particle that has a closest approach less than r_c, which we mark as a collision.

The strength of the collisions in our test-particle framework (characterized by the Lorentz factor of the colliding particles in the zero-momentum frame of the collision) gives a first indication of the expected shock strengths in the corresponding fluid system and, hence, is our best handle on the possibility of observable electromagnetic signatures. We obtain the Lorentz factor of each colliding particle, in locally Minkowskian coordinates, as follows. Given two colliding particles A and B, first we compute the scalar product of the proper 4 velocity u_A^μ of particle A with the proper 4 velocity u_B^μ of particle B. Note that regardless of the original coordinates in which the product is computed, it exactly equals the negative of the Lorentz factor of particle A in the rest frame of particle B (as it would be calculated in locally Minkowskian coordinates). That is,

$$u_A^\mu u_B^\nu g_{\mu\nu} = u_A^{\mu'} u_B^{\nu'} g'_{\mu\nu} = -u_A^{0'} \qquad (1)$$

because $u_B^{\mu'} = \delta_0^\mu$ and $g'_{\mu\nu} = \eta_{\mu\nu}$, where the primes refer to the inertial frame of particle B. We then transform to the center-of-momentum frame by solving for the Lorentz factor γ_{com} characterizing the Lorentz transformation matrix that transforms $u_A^{\mu'}$ and $u_B^{\mu'}$ to $u_{A(com)}^\mu$ and $u_{B(com)}^\mu$ such that

$$u_{A(com)}^0 = u_{B(com)}^0 = \gamma_{com}, \ \ u_{A(com)}^i = -u_{B(com)}^i. \qquad (2)$$

We finally obtain

$$\gamma_{com} = \sqrt{\frac{1}{2}\left(1 - u_A^\mu u_B^\nu g_{\mu\nu}\right)}. \qquad (3)$$

3. RESULTS AND DISCUSSION

Our main results are displayed in Figures 1–4. In Figures 1 and 2, with initially orbital and isotropic particle velocities respectively, we show the maximum Lorentz factor of a collision between any two particles as a function of time, for several different setups including one with an isolated Schwarzschild black hole for comparison. Because collisions do not affect particle trajectories in our calculations (i.e., the geodesic paths are unaltered), we expect these to be upper bounds on the true Lorentz factors of collisions given that in the MHD situation realized by nature there will be dissipation of relative speeds through collisions.

In Figures 1 and 2, the top panel shows the control case, in which the particles orbit around a solitary black hole. The other two panels involve nonspinning (middle panel) and spinning (bottom panel) binaries. The merger in these cases, defined by the detection of a common apparent horizon, takes place at $t = 0$.

Our control case shows as expected that after a short initialization phase the maximum Lorentz factor is roughly constant. Here the highest-speed collisions are between particles that have both fallen close to the horizon and thus have acquired speeds considerably in excess of their initial orbital speeds. Given that the particles have a "thermal" velocity distribution in which the random speed is comparable to the orbital speed, a reasonable fraction of particles is captured by the black hole.

In the binary runs, the varying accelerations caused by the binary motion are expected to alter significantly the energy and
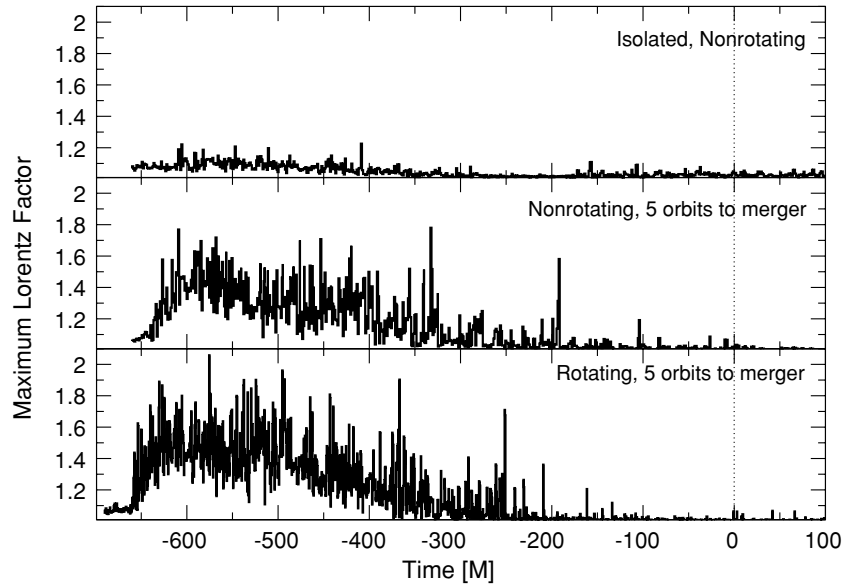
Figure 1. Maximum Lorentz factors of collisions between particles as a function of time before merger for initial velocities that include an orbital velocity plus a random isotropic component. The three panels are for the following cases: (top) isolated nonrotating black hole, (middle) two spinless black holes, merging in approximately five orbits, and (bottom) two black holes each with spin parameters of $a/m = 0.8$, merging in approximately six orbits. In all cases both black holes have mass m. The data have been aligned with respect to the time axis such that the common apparent horizon is first detected at $t = 0$. M is the total system mass.
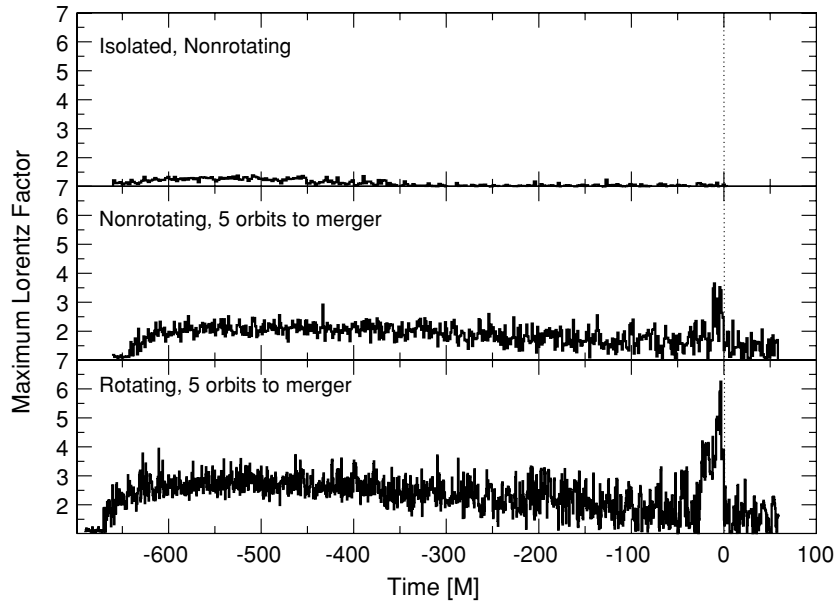

Figure 2. Same as Figure 1 but for particles whose initial velocity is purely random and isotropic, with no net orbital component. From this figure we note that (a) in both binary cases there is a clear maximum in the Lorentz factor just prior to merger, whereas (as expected) the isolated case has a steady Lorentz factor, and (b) in the spinning case, the collisions throughout and near merger are more violent than in the nonrotating runs.

angular momentum of particles within ∼2 binary orbital radii, just as in the Newtonian slingshot analogue. More rapid orbits therefore are expected to lead to higher-speed collisions and (as is evident in Figure 4) faster outflows, with the effect maximized shortly before merger because this is when the orbital speeds are greatest.

Examining Figure 2 we find that these expectations are largely met for the isotropic particle velocities. There is indeed a strong peak in the maximum collision Lorentz factor just before merger. This peak is highest when the holes are rotating, as is reasonable because for the aligned spin configuration the holes can get closer and thus orbit faster before they plunge together. The

Lorentz peaks are in all cases considerably higher than in the isolated hole runs, which might lead us to cautious optimism that this phase might be observably different for a binary merger than for an isolated hole. However, in the case of particles with initial average velocities that are approximately orbital, the central region of the disk remains evacuated near the time of merger, as the particles have found quasi-stable orbits further out. In this case, there is no discernible merger signature, as seen in Figure 1. We conjecture that the inclusion of viscosity would push orbiting matter closer toward the binary, resulting in energetics between the above two extremes, and recovering a merger signature. If this is confirmed by future detailed MHD calculations, it may
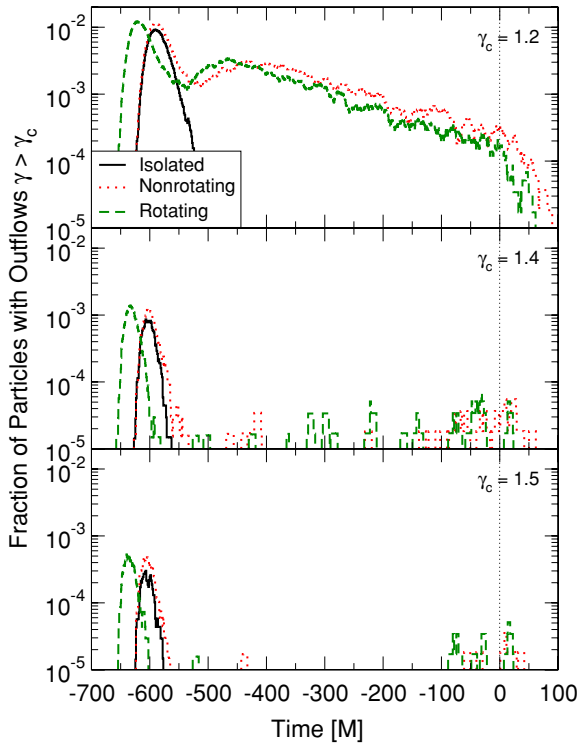
Figure 3. Fraction of particles with positive radial velocities in a shell with surfaces at 25 M and 30 M with a corresponding Lorentz factor greater than (top to bottom) 1.2, 1.4, 1.5, comparing the cases with an isolated spinless black hole (solid black), a binary with spinless equal-mass black holes (dotted red), and a binary with equal-mass black holes with spins of $a/m = 0.8$ (dashed green). On the scale plotted, one particle gives a fractional value of 1/75,000 or 1.3×10^{-5}.

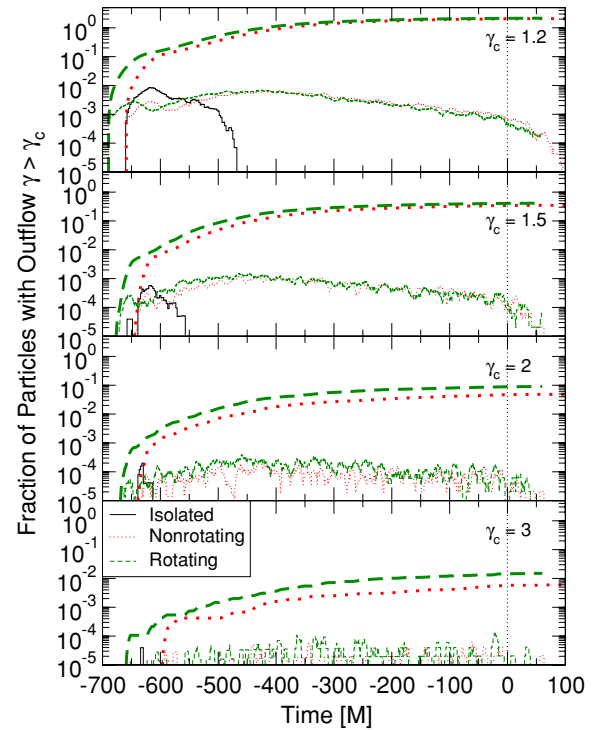(A color version of this figure is available in the online journal.)

Figure 4. Same as Figure 3 but for the case of particles having only initial random velocities and Lorentz factors greater than (top to bottom) 1.2, 1.5, 2, and 3. Also shown are the cumulative sums of these fractions.

(A color version of this figure is available in the online journal.)

provide another way to identify an electromagnetic counterpart to the gravitational waves from a binary supermassive black hole merger.

In examining the locations of the highest energy collisions which constitute the merger signature described above, we find that most of them occur within ∼0.1–0.5 M outside the apparent horizon surfaces (in contrast, the radius of the apparent horizon around each black hole is ∼0.2 M.) Although the apparent horizon may differ from the event horizon depending on the coordinates and dynamics of the black holes, the apparent horizon finding algorithm developed by Thornburg (2004), which we use, typically gives close agreement with event horizons during most of a binary black hole simulation. We therefore expect significant energy from these collisions to escape to observers at arbitrary distances. However, again, more definitive verification must await simulations incorporating electromagnetic fields.

Other features of these figures are, we believe, artifacts of the limitations of our simulation. For example, even with isotropic particle velocities, in both the spinning and the nonspinning binary runs, we see an overall decrease in the maximum Lorentz factor of collisions during inspiral. We suspect that this is because our setup includes no angular momentum transport between particles, hence as the simulation progresses we run out of particles that would naturally plunge toward the holes and produce very high speed collisions.

In Figures 3 and 4, we explore the outflow Lorentz factor, measured in a shell of thickness 5 M with its inner surface equal to initial disk outer radius of 25 M. Particularly in the case

of isotropic particle velocities, because we have a significant random speed in our thick disks, the isolated hole has some fraction of particles that move rapidly outward, but we see that the fraction of such particles is (as expected) very small compared to those of the binary runs where particles are flung out via a slingshot effect.

The main meaningful difference, in Figure 4, is between the spinning and nonspinning binary simulations. At a given time before merger, due to spin–orbit coupling in the spinning case, the holes are orbiting faster than in the nonspinning case. As a result, the slingshot effect is stronger at all times from merger, and near merger itself the speeds are higher yet. It is also possible that frame-dragging due to spin plays a more direct role, by increasing the ejection speeds in a manner akin to an eggbeater. At the highest speeds seen, there is no parallel for the isolated black hole run. Depending greatly on the nature of the interactions of the outflow (e.g., the development of shocks or the initiation of Fermi acceleration), it is possible that high-energy radiation such as gamma rays may be produced in ways that make it possible to discriminate between single and binary black holes, or even possibly between slowly rotating and rapidly rotating black holes.

In summary, our exploratory calculations represent a step toward realistic simulations of the accretion flow near binary supermassive black holes close to merger. Under certain conditions, our results show differences between single and binary black holes, and between nonrotating and rapidly rotating binary black holes, which is encouraging for future observations. As such, they motivate more realistic hydrodynamic and MHD calculations, which will be our next steps. If some of the qualitative differences found in our test particle calculations (with isotropically distributed velocities) are maintained in future work with fluids, this will imply prompt electromagnetic signatures that

can be correlated with gravitational radiation signals detected by the space-based *Laser Interferometer Space Antenna* (Baker et al. 2007; Lang & Hughes 2009), allowing precise cosmological probes and constraints on dark energy (Arun et al. 2009) and even testing fundamental principles such as the relative speed of propagation of photons and gravitational waves.

REFERENCES

Armitage, P. J., & Natarajan, P. 2002, ApJ, 567, L9
Arun, K. G., et al. 2009, Class. Quantum Grav., 26, 094021
Baker, J. G., Boggs, W. D., Centrella, J. M., Kelly, B. J., McWilliams, S. T., & van Meter, J. R. 2008, Phys. Rev. D, 78, 044046
Baker, J. G., Centrella, J. M., Choi, D.-I., Koppitz, M., & van Meter, J. R. 2006, Phys. Rev. Lett., 96, 111102
Baker, J. G., et al. 2007, LISA: Probing the Universe with Gravitational Waves, http://www.lisa-science.org/resources/talks-articles/science/lisa_science_case.pdf
Balbus, S. A., & Hawley, J. F. 1991, ApJ, 376, 214
Baumgarte, T. W., & Shapiro, S. L. 1998, Phys. Rev. D, 59, 024007
Bode, N., & Phinney, S. 2007, APS Meeting Abstracts, 1010
Brandt, S. R., & Brügmann, B. 1997, Phys. Rev. Lett., 78, 3606
Brown, J. D., & Lowe, L. L. 2005, J. Chem. Phys., 209, 582
Campanelli, M., Lousto, C. O., Marronetti, P., & Zlochower, Y. 2006, Phys. Rev. Lett., 96, 111101
Chang, P., Strubbe, L. E., Menou, K., & Quataert, E. 2009, arXiv:0906.0825
Dotti, M., Salvaterra, R., Sesana, A., Colpi, M., & Haardt, F. 2006, MNRAS, 372, 869
Haiman, Z., Kocsis, B., & Menou, K. 2009a, ApJ, 700, 1952
Haiman, Z., Kocsis, B., Menou, K., Lippai, Z., & Frei, Z. 2009b, Class. Quantum Grav., 26, 094032
Hughes, S. A., & Holz, D. E. 2003, Class. Quantum Grav., 20, 65
Ichimaru, S. 1977, ApJ, 214, 840
Imbiriba, B., Baker, J. G., Choi, D.-I., Centrella, J. M., Fiske, D. R., Brown, J. D., van Meter, J. R., & Olson, K. 2004, Phys. Rev. D, 70, 124025
Kocsis, B., Frei, Z., Haiman, Z., & Menou, K. 2006, ApJ, 637, 27
Kocsis, B., Haiman, Z., & Menou, K. 2008, ApJ, 684, 870
Kocsis, B., & Loeb, A. 2008, Phys. Rev. Lett., 101, 041101
Lang, R. N., & Hughes, S. A. 2009, Class. Quantum Grav., 26, 094035
Lippai, Z., Frei, Z., & Haiman, Z. 2008, ApJ, 676, L5
Megevand, M., et al. 2009, Phys. Rev. D, 80, 024012
Milosavljević, M., & Phinney, E. S. 2005, ApJ, 622, L93
Narayan, R., & Yi, I. 1994, ApJ, 428, L13
O'Neill, S. M., Miller, M. C., Bogdanovic, T., Reynolds, C. S., & Schnittman, J. D. 2009, ApJ, 700, 859
Palenzuela, C., Anderson, M., Lehner, L., Liebling, S. L., & Neilsen, D. 2009, Phys. Rev. Lett., 103, 081101
Phinney, E. S. 2007, APS Meeting Abstracts, 7002
Phinney, E. S. 2009, arXiv:0903.0098
Rees, M. J., Begelman, M. C., Blandford, R. D., & Phinney, E. S. 1982, Nature, 295, 17
Schnittman, J. D., & Krolik, J. H. 2008, ApJ, 684, 835
Shibata, M., & Nakamura, T. 1995, Phys. Rev. D, 52, 5428
Shields, G. A., & Bonning, E. W. 2008, ApJ, 682, 758
Thornburg, J. 2004, Class. Quantum Grav., 21, 743
van Meter, J. R., Baker, J. G., Koppitz, M., & Choi, D.-I. 2006, Phys. Rev. D, 73, 124011